Геология и геофизика, 2022, т. 63, № 7, с. 1035—1048

УДК 550.34+622.241

ОПРЕДЕЛЕНИЕ ПОТЕНЦИАЛА ПЛАСТА-КОЛЛЕКТОРА В МЕЖСКВАЖИННОМ ПРОСТРАНСТВЕ НА ОСНОВЕ КОМПЛЕКСНОГО ГЕОЛОГО-ГЕОФИЗИЧЕСКОГО ИССЛЕДОВАНИЯ С УЧЕТОМ СЕЙСМИЧЕСКИХ АТРИБУТОВ И ДАННЫХ ДОБЫЧИ

А.К Жумабеков[1,2], Д. Лиу[1], В.С. Портнов[2], С. Вэй[3], С. Чэн[3]

[1]*State Key Laboratory of Petroleum Resource and Prospecting in China University of Petroleum, Fuxue road 18, Changping, Beijing, 102249, China*

[2]*Karaganda State Technical University, N. Nazarbayev Avenue 56, Karaganda, 100027, Kazakhstan*

[3]*BGP inc., China National Petroleum Company CNPC, Fanyang West Road 189, Zhuozhou, Hebei, 072751, China*

Динамическая модель сейсмических, геологических и гидродинамических характеристик коллектора является основным инструментом, используемым для оценки потенциала бурения новых уплотняющих скважин. Статическая геологическая модель основана на скважинных данных в сочетании с анализом динамики добычи. Данная модель используются для определения реконструкции и корректировки новых мест бурения; однако такие модели редко включают сейсмические данные. Следовательно, трудно контролировать изменения в геологических моделях между скважинами, что приводит к необходимости прослеживания конфигурации расположения скважин и прогнозируемых результатов, которые, в свою очередь, могут описывать неполную картину ситуации. Чтобы улучшить разработку скорректированных участков с точки зрения содержания в них остаточной нефти, мы разработали новый комплексный анализ, сочетающий в себе статическое моделирование отложений, в том числе анализ микрофациальности (среди других коллекторских и сейсмических свойств), с поведением добычи. В данной работе приводится новый метод, включающий в себя следующее: (1) установление благоприятных областей для статического геологического анализа; (2) изучение потенциала заканчивания скважин и состояния непроизводящих скважин; (3) проведение межскважинного анализа с использованием сейсмических и седиментационных данных; (4) определение потенциальных участков, ограниченных сейсмическими и геологическими исследованиями, а также начальным уровнем добычи месторождения; (5) внесение предложений в план разработки новых скважин.

Геологическая модель, осадочные фации, сейсмические атрибуты, разработка скважин, остаточная нефть

INTEGRATING THE GEOLOGY, SEISMIC ATTRIBUTES, AND PRODUCTION OF RESERVOIRS TO ADJUST INTERWELL AREAS

A.K. Zhumabekov, Z. Liu, V.S. Portnov, X. Wei, X. Chen

Dynamic models of the seismic, geological, and flow characteristics of a reservoir are the main tool used to evaluate the potential of drilling new infill wells. Static geological models are mainly based on borehole data combined with dynamic analyses of production dynamics. They are used to determine the redevelopment of and adjustments to new drilling locations; however, such models rarely incorporate seismic data. Consequently, it is difficult to control the changes in geological models between wells, which results in the configuration of well positions and predicted results being less than ideal. To improve the development of adjusted areas in terms of their remaining oil contents, we developed a new integrated analysis that combines static sediment modelling, including microfacies analysis (among other reservoir and seismic properties), with the production behaviour. Here, we illustrate this new process by (1) establishing favourable areas for static geological analysis; (2) studying well recompletion potential and the condition of nonproducing wells; (3) conducting interwell analyses with seismic and sedimentary data; (4) identifying potential sites constrained by seismic and geological studies, as well as initial oilfield production; (5) providing suggestions in a new well development plan.

Reservoir geological model, sedimentary facies, seismic attributes, well development, remaining oil

INTRODUCTION

Here, we present a case study of an oil field in the Mangyshlak Basin of West Kazakhstan, which has many operational reservoir intervals. Previous studies in the South Mangyshlak subbasin have indicated that the Middle Jurassic reservoir interval may be subdivided into thirteen productive units – I (Callovian) to XIII

✉e-mail: zhak28@gmail.com
DOI: 10.15372/GiG2021168

(Aalenian). Fine- to medium-grained fluvial (channel) sandstones with typical permeabilities of 6–115 mD (maximum: 239 mD) constitute the main reservoir facies; reservoir quality is severely impaired by the amount of clay and carbonate cement, which may reach 50% of the bulk rock volume regionally (Ulmishek, 2001). The reservoir is strongly layered, with numerous lacustrine to shallow marine shale layers occurring both between and within the productive units, effectively partitioning the stratigraphic section and giving rise to multiple hydrocarbon–water contacts. Reservoir units are internally heterogeneous with only moderate vertical connectivity and unidirectional lateral connectivity dictated by channel orientation. An interpretation of a newly acquired three-dimensional (3-D) seismic survey in the northwest of the field was scheduled to guide new drilling activities, beginning in early 2008; however, data on the drilling status are currently unavailable.

To further petroleum exploration in this basin, it is necessary to re-evaluate its constituent reservoirs. Reservoir redevelopment planning combined with seismic correlations can be used to predict the remaining volume and distribution of hydrocarbons, thereby promoting petroleum exploration (Gunter et al., 1997; Carter, 2003; Tang et al., 2019). However, no studies involving the seismic correlation of the reservoirs in the Mangyshlak Basin have been conducted. Comprehensively determining the remaining oil in this basin will therefore require correlating seismic attributes and systematically analysing the geological and fluid conditions. In this study, seismic and geological facies, along with the dynamic operating conditions, were considered for the development interval of the target horizon (J-III) to establish the remaining oil potential. We first evaluated the primary favourable zones, so that our analyses of seismic attributes were conducted in areas with high effective thicknesses, favourable sedimentation, and large potential remaining oil volumes. Secondly, the dynamic properties were defined, the study of which focused mainly on the following parameters: oil and water migration in areas with little restriction by the well grids, areas with limited depletion, and areas with low water cuts after development. Here, we promote the further opportunities for find remaining oil through drilling new wells and re-invigorating idle wells (Arslan et al., 2019).

GEOLOGICAL SETTING AND STATIC ANALYSIS

The Mangyshlak Basin is located on the eastern coast of the Middle Caspian Sea, primarily in West Kazakhstan (Fig. 1). The basin continues into Uzbekistan and Turkmenistan in the east and south, respectively. The structural terrace on the northern margin of the South Mangyshlak subbasin in the Middle Caspian Basin (Kiritchkova et al., 1983) hosts the majority of the oil and gas fields (Soloviev et al., 2017). The Middle Caspian Basin (Kazhegeldin, 1997; Effimov et al., 2001; Lechner et al., 2016) is floored by continental terrane that accreted onto the southern margin of the Eurasian Plate during the Permian. Its sedimentary fill consists of up to 12 km of predominantly Mesozoic strata (Aliyeva, 2009) in a large inverted rift.

The structural development of the Mangyshlak subbasin began during the late Permian–Triassic, when rifting created a large west–northwest (W–NW) graben over the Mangyshlak uplift zone. It was initially filled with a thick interval of clastic continental sediments, transitioning to a marine sedimentary basin with local volcanic horizons in the Middle–Late Triassic. The uppermost Lower Triassic–Middle Triassic shales are the likely source of most of the hydrocarbons in in South Mangyshlak fields (Ulmishek, 1990, 2001).

To visualise different sedimentary environments and their representative facies (Zudakina et al., 1981), core and logging data, petrophysical parameters (Gunter et al., 1997; Pennington, 1997; Zhang et al., 2016), reservoir summaries (Berkhout, 1993; Walls et al., 2004), and sedimentary facies types are needed; the separations among the facies in individual wells are marked on seismic profiles (Posamentier, 2000; Harilal et al., 2008; Avseth et al., 2010; El-Mowafy et al., 2016) and geological maps (Wu et al., 2014; Tang et al., 2019). To improve the continuity of sand bodies, we combine microfacies characteristics and seismic data with the root mean square (RMS) seismic attribute (Brown, 1996; Chopra et al., 2005, 2014). Furthermore, to identify the main productive zones and potential areas with remaining oil, the initial oil production rates, water cuts, and cumulative productions of well were correlated with the current information.

Reservoir architecture

Oil and gas accumulations occur in very heterogeneous reservoirs due to their deposition in fluvial channels and associated facies. Each of the thirteen productive Middle Jurassic reservoir units of the South Mangyshlak subbasin typically comprise two to eight discontinuous sandstone layers. The oil pay in individual reservoir units is 1.3–21.2 m and gas pay is 2–14.4 m (Kazhegeldin, 1997). Continuous mudstone layers, typically 1–20-m-thick, separate the reservoir units, which act as separate flow layers. Vertical connectivity within reservoir units ranges from moderate to poor, owing to the moderate abundance of mudstone layers. Lateral connectivity is higher because of the braided channel belts (200–700-m-wide in the nearby Uzen Field) but are unidirectional and in line with the dominant SW-trending channel orientation.

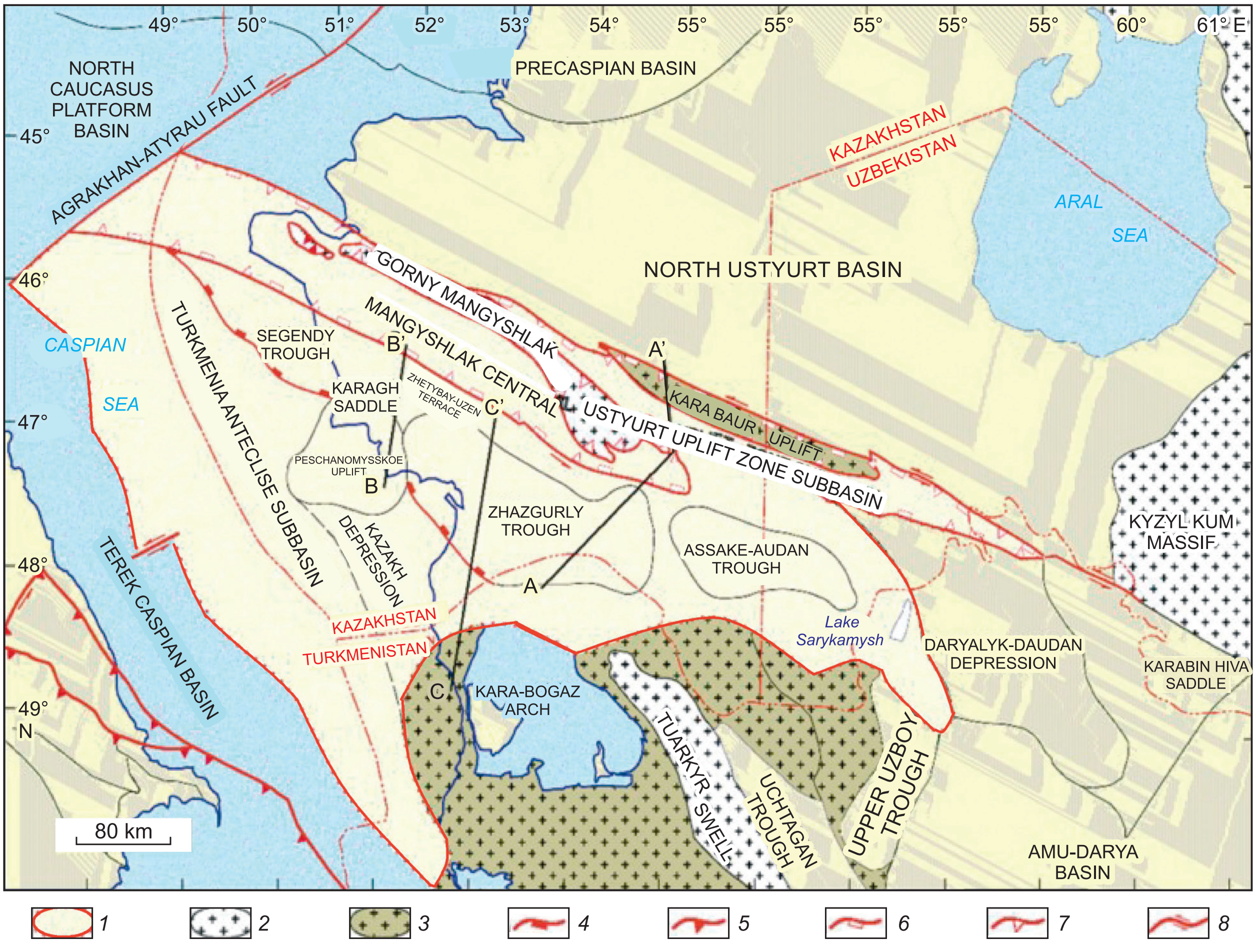

Fig. 1. Location of the Mangyshlak Basin.

1 – basin limit, *2* – basement outcrop, *3* – basement high, *4* – normal fault, *5* – reverse fault, thrust fault, *6* – reactivated normal fault, *7* – reactivated thrust, *8* – strike-slip fault.

Sedimentary facies

Analysing seismic and log phases allows us to predict the distribution of sedimentary microfacies (Muruthy and Ghosh, 2018) per reservoir interval in a study area. Horizons J-I to J-XI were interpreted as delta front deposits, with interbedded sands and mud, an overall fine grain size and multi-stage upward-coarsening reverse sequence. The submarine distributary channel is the main reservoir facies, with the mouth bar and distal bar serving as secondary reservoirs. Horizons J-XII to XIII were interpreted as braided channels with thick, clean sand layers, coarse particle sizes, and a stable depositional history; they are the main reservoir rocks in these horizons.

Depositional heterogeneity greatly impacts the distribution and areal extent of sedimentary microfacies. From the map of facies in horizon J-III (Fig. 2), it is evident that the sediment was sourced from the north, with four 4-branched deltas, and the channel sand bodies spread in a wide strip in the near N–S strike direction. The width of the four zones of channel development in the north ranges from 3 to 7 km and these represent the main reservoirs. In the south, the sand bodies of distal estuarine sand bars are developed and serve as secondary reservoirs.

Reservoir properties

The reservoirs of the studied oilfield consist of poorly- to moderately-sorted, fine- to medium-grained arkoses and sublitharenites cemented by clays and carbonates. Regionally, clay content may reach up to 50% of the bulk rock volume (Ulmishek, 2001). Mean permeabilities are low (6–115 mD, maximum: 239 mD) and

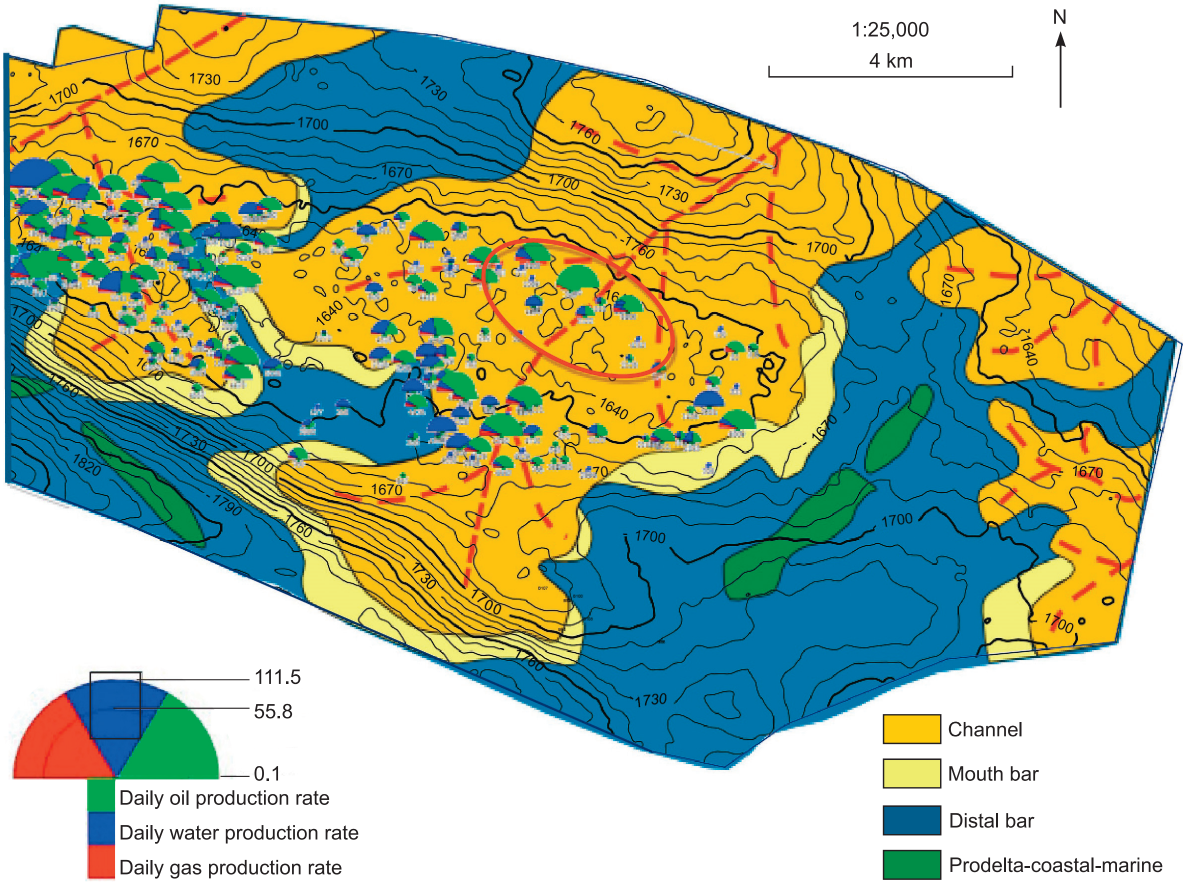

Fig. 2. Overlay map of the initial productivity, sedimentary microfacies, and structure of horizon J-III.

decline drastically with increasing clay content. Thick, coarser-grained channel sandstones are characterised by lower clay contents and therefore higher permeabilities. Median porosities range from 16–22% (Kazhegeldin, 1997). A dual-porosity system exists due to the secondary intergranular pores resulting from the dissolution of cements, and intragranular microporosity is formed by the partial leaching of feldspars (Smale et al., 1997). The distribution of larger, intergranular pores controls the overall permeability, which consequently shows no relationship with total porosity (Zudakina et al., 1981). Initial water saturations are relatively high (30–45% for oil and 38–44% for gas), likely due to the retention of water via micropores.

The results of core analyses in the study area revealed that the medium porosity in Jurassic deposits at the oilfield ranges from 14.7–19.8%. In this study, the Median porosity was determined for the oil-bearing strata, and the highest percentage was found in the J-III horizon (19.8%). Meanwhile, the porosity of the J-XI oil horizon was relatively low (14.7%). The permeability of the 13 oil-bearing formations in the Jurassic sediments was highly variable, averaging between 42 and 116 mD. The mean permeability along the J-V production horizon had the highest value (119 mD); that of the J-XIII horizon was also quite high, at 117 mD. Compared with the aforementioned horizons, the mean permeabilities of horizons J-X and J-XI were relatively low, 43 mD and 44 mD, respectively. Thus, the 13 oil-bearing units are terrigenous reservoirs (sandstones) with medium porosity and medium permeability. The reservoirs within the productive horizons, J-XII to J-XIII, are represented by sandy coarse-grained sediments, and their median porosity may be underestimated relative to the overlying productive horizons, though the mean permeability is higher.

Application of seismic attributes

The elastic properties of rocks depend on the conditions of sedimentation (sedimentation trends), diagenetic processes (for example, the formation of cement), on the type and properties of the type of fluid contained in the pores. Typically, these properties follow certain trends with increasing depth. The methodology used in this study and correlation allows to include depth trends in a quantitative form in the forecast and classification of lithotypes and fluids based on the results of inversion of seismic data. At the same time, the statistical scatter of elastic properties is taken into account when assessing the forecast accuracy.

The inversion was performed in the pre-stack version, *V*p, *V*s, AI, SI, *V*p/*V*s. The inversion parameters themselves and the scaling of the results were determined by reference to existing wells and statistical selection of a low-frequency model. Synchronous inversion with a low-frequency model has been performed. It was decided to expand the number of wells for the low-frequency model, which implies a more detailed background model and a more accurate classification of the inversion results. The application of the principles of Bayesian classification allows the entire set of known geological information to be included in the probabilistic forecast, in the assessment of accuracy and in the forecast of risks.

Inversion results. Like each quantitative interpretation method, the applicable approach depends both on the quality of the input data (completeness and quality of well curves; their reliable petrophysical interpretation; optimal parameters of field recording of seismic data; their qualitative digital processing), and on the elastic properties of rocks themselves (mainly, physical dismemberment of different lithotypes). However, quantifying depth trends when interpreting seismic data significantly increases their predictive value and reduces the uncertainty of the results.

In this case, the created probability distribution functions of elastic properties are used in order to assign the most probable lithotype (aquiferous sandstone, oil sandstone, pure clay, clay containing coal, volcanic rock, etc.). The seismic attribute in area reflects well the characteristic of lithological variability. According to the *V*p/*V*s attribute, it was noted in the formation by area that in the central and eastern parts there is a high attribute anomaly expressed by "red" tones, respectively, "blue" tones are present between the eastern and central parts, which is, in its turn, a zone of lithological variability. This significantly coincides with the drilling data therefore, using the *V*p/*V*s attributes in terms of area, it is possible to describe the zone of lithological variability, which provides the prerequisites for the analysis of water oil contact. Illustrated the color response spectrum clearly describes the red sandy bodies and their near-boundary discontinuous values in the central part of the section. Below the investigated trend, an insignificant yellow, green response was revealed as less porous bodies where clay-containing rock material is located. In the red areas of sandy porous bodies, there are zones of increased water cut due to high fluid content with places of potential remaining oil content.

In the process of selecting individual wells with seismic attributes and inversion results, we mapped the sedimentary facies of these objects based on GeoEast software. Seismic attributes were selected and sensitivity analyses were performed. Different types of surface attributes (i.e., amplitude, frequency, phase, wave type) and drilling data were analysed and compared. The RMS attribute is suitable for countering the anomalous zones in the study area (marked in red in Fig. 3). The seismic attributes were then analysed, including the reservoir RMS

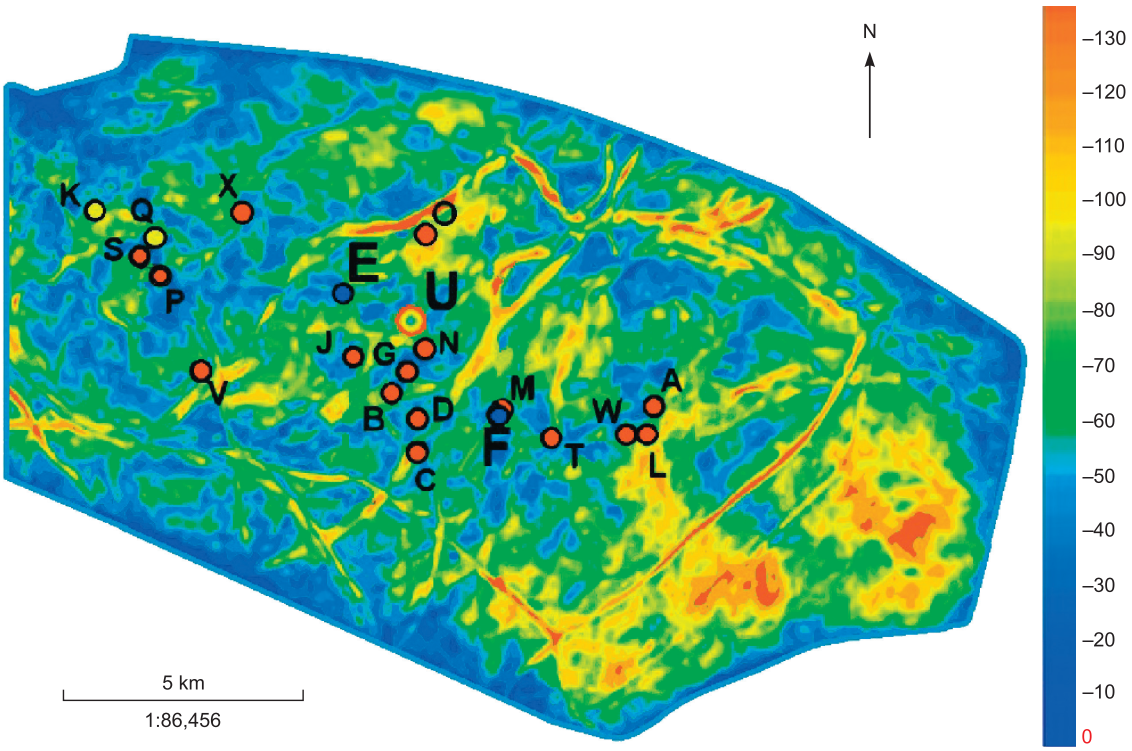

Fig. 3. Overlay map of the initial productivity of recompleted wells from the underlying horizon and RMS attributes of J-III. Well labels correspond to those shown in Table 1.

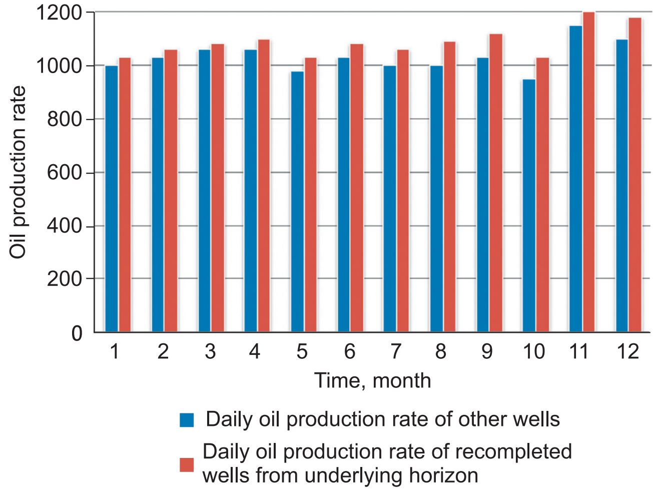

Fig. 4. Production contributions of recompleted wells from the underlying horizon and other wells of J-III.

reflectivity and data on the well operation dynamics, and sedimentary microfacies characteristics were studied by area. Wells with high initial productivities were primarily located in the main reservoir – a branched channel with strong amplitudes (displayed in yellow in Fig. 3). The sand body in the main channel is well developed and characterised by favourable petrophysical properties and low heterogeneity (Cao et al., 2005). Wells with low initial productivities were predominantly distributed beyond the edges of the channels (shown in green and blue in Fig. 3). These areas contain thin sand bodies with poor connectivity and strong heterogeneity.

EXPERIMENTAL WORK-FLOW AND METHODOLOGY

Well recompletion potential

As a shallow horizon, J-III has been drilled in nearly every well throughout the region, and the operating well stock consists of 100 production and 42 injection wells across all reservoir layers. If J-III is to be redeveloped, the current dedicated well stock is insufficient and more wells will be needed. The recompletion of old wells originally drilled to develop deeper intervals should allow us to economically and quickly resolve this problem. In horizon J-III, there are 24 recompleted wells from the underlying horizon (Table 1), of which nine are in the west and 15 are in the east; the maximum daily production rate of a single well is 188.26 bbl/d.

From the overlay map of recompleted wells and RMS seismic attributes (Fig. 3), high-production wells were found to correlate with stronger amplitudes, which indicates that seismic attributes can be used to predict reservoir properties. The cumulative oil production from recompleted wells from the underlying horizon of J-III reached 1.11 kbbl, with a daily oil production rate 369.06 bbl/d – equalling 8% of the total production of this horizon (Fig. 4). Recompleting wells from the underlying horizon has therefore had a positive effect.

Currently, the percentage of idle wells in the study area is high, and the utilisation rate of old wells is low. Over 90% of the wells have been shut-in due to high water cut and low production rates. Since the proportion of inactive wells in the deepest reservoir intervals, J-IX to J-XIII, is higher than 65% (Table 2), there are many recompletion candidate wells for shallower intervals that may increase their utilisation rates. A large complex of sand bodies interpreted in logging data in the eastern part of horizon J-III (Fig. 5), along with bright seismic amplitudes and the modelled remaining oil potential. From the results shown in this figure, we recommend increasing the reservoir throughput rate of J-III and the utilisation rates of old wells.

Table 1. **Start time and initial oil production rate of the J-III horizon**

Well	Start time of utilisation	Initial production rate J-III (bbl/day)
A	January, 2017	3.96
B	September, 2017	1.89
C	July, 2017	1.64
D	July, 2017	1.51
E	September, 2017	1.26
F	August, 2017	0.63
G	April, 2017	4.78
H	December, 2017	1.26
I	July, 2017	17.67
J	June, 2017	25.98
K	December, 2017	78.56
L	July, 2017	33.15
M	May, 2017	23.71
N	April, 2017	59.63
O	April, 2017	32.71
P	April, 2017	57.62
Q	October, 2017	67.68
R	May, 2017	81.14
S	February, 2017	57.05
T	August, 2017	54.53
U	August, 2017	188.26
V	November, 2017	35.92
W	July, 2017	12.89
X	July, 2017	22.58

Table 2. **Conditions of wells by reservoir interval**

Target horizon	Well stock of producing wells	Historical well stock of producing wells	Well stock of shut wells	Well stock of injection wells	Historical well stock of injection wells	Ratio of historical producing and shut wells, %
J-II	0	2	2	0	0	100
J-III	18	100	31	42	32	30.69
J-IV	25	40	18	5	6	44.44
J-V	13	200	123	20	95	61.49
J-VI	10	150	91	18	89	60.77
J-VII	20	30	12	2	4	39.39
J-VIII	15	330	213	35	123	64.68
J-IX	44	120	93	15	28	77.32
J-X	13	400	291	48	143	72.83
J-XI	36	50	34	10	14	67.27
J-XII	6	350	295	24	101	84.21
J-XIII	5	80	76	1	1	95.33
Total	211	993	506	203	404	50.99

Dynamic analysis

Analyses of the water cut conditions of production wells within one reservoir interval and between neighbouring wells revealed the water cut amount of these wells varied widely. We took one group of wells in the southern part of horizon J-III as an example (Fig. 6) to analyse the operating conditions of each well and found that wells Y-3, Y-7, Z-2, Z-4, and V had low water cuts and high oil production rates, while neighbouring wells had high water cuts. From the results of seismic inversion, highly watered wells, such as Y-5, X-4, and X-7, were primarily found in the areas of sand body enrichment. In cross-sectional seismic inversions (Zabihi Naeini and Exley, 2016), low-water-cut wells, Z-4, Y-7, V, and Y-3, were located on the edge of the sand body and in the discontinuous area, and the remaining oil was relatively highly concentrated. Therefore, this is the main target area for drilling new wells and developing residual oil (Fig. 7).

The most critical step for the joint impedance and facies-based inversion technique was to define depth trends for each facies. From these per-facies depth trends equivalent low frequency models are generated, an essential input to the algorithm. The depth trends, where the main facies are classified. The various layers types into different facies types was a critical factor to improve the inversion accuracy. Facies based seismic inversion, a great tool to provide significant advantages over more conventional impedance inversion techniques. When facies-based inversion is combined with broadband data and appropriate broadband well tie techniques the resulting classified facies output provides a result ideally suited for geological interpretation and the generation of static and dynamic reservoir models. The inversion technique successfully provides a better facies correlation with calibration wells. Also inverts for an optimum low frequency model – thereby removing one of the most significant sources of error in more conventional simultaneous inversion techniques, where a low frequency model is an input, not an output. Therefore, it reduces interpretation burden by producing facies output akin to a geo-cellular model. Allows a full range of potential sensitivities to be explored therefore exploring the implications of inversion error.

Integrated analysis of geology, seismic attributes, and production performance

There is a wide distribution in the current water cut of the horizon J-III production wells, as well as a large proportion of high-water-cut wells. It can be seen that the water cut is the highest in the high-productivity wells of the main channel bodies, while lower productivity wells along the edge and lateral sides of the channel have lower degrees of flooding and thus higher potentials for remaining oil. Moreover, the cumulative production by well in horizon J-III is relatively high in the west and low in the east (Fig. 8). Production wells on the lateral side of the channel also have low cumulative productions and low water cut levels. Consequently, in the eastern part and the lateral side of the channel, J-III has the highest potential for remaining oil, including a part with a low degree of involvement. Considering these results, horizon J-III is the key layer for tapping potential phase zones, as it has the following favourable conditions: relatively low oil recovery, substantial lateral variability in the reservoir, and regionally low water production.

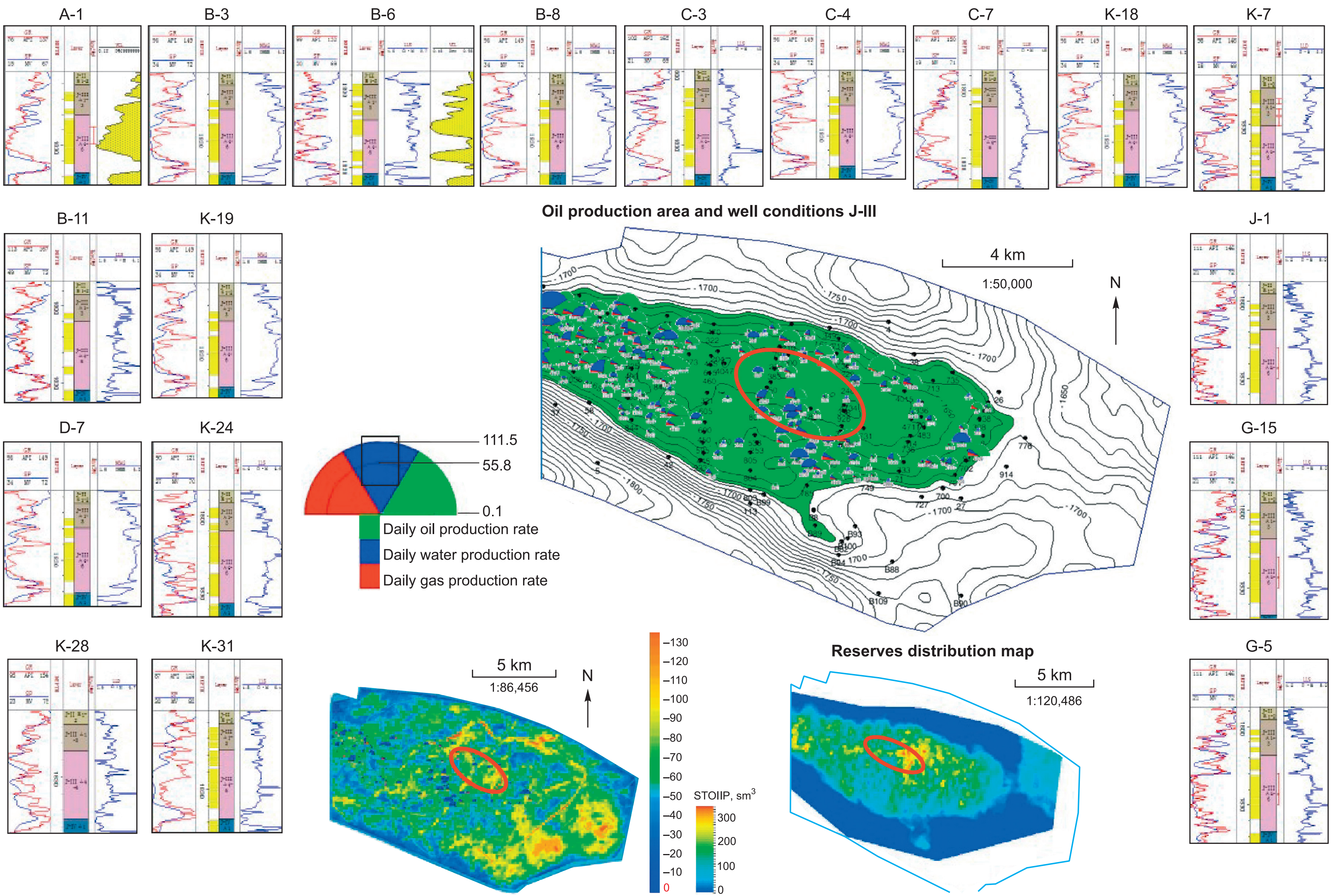

Fig. 5. Map of the distribution of idle wells in the study area with remaining oil potential.

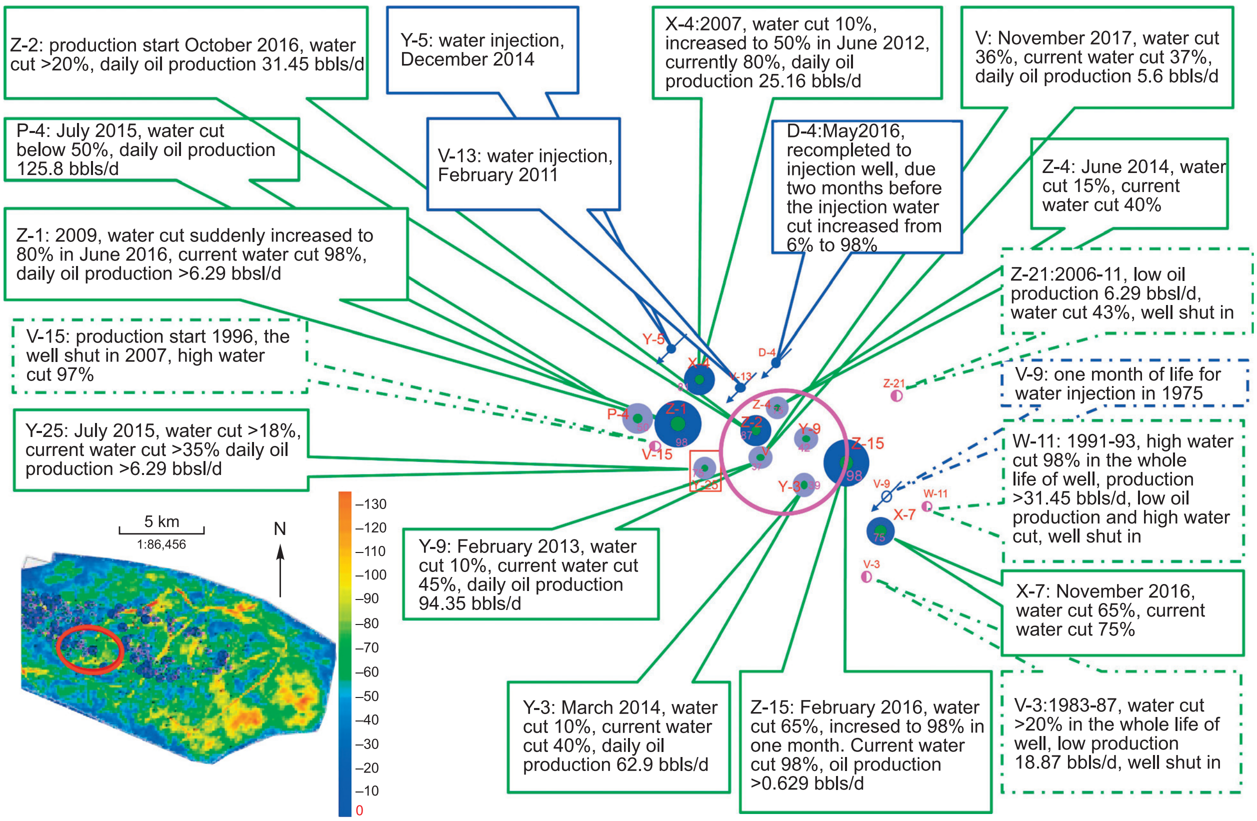

Fig. 6. Dynamic analysis of well groups.

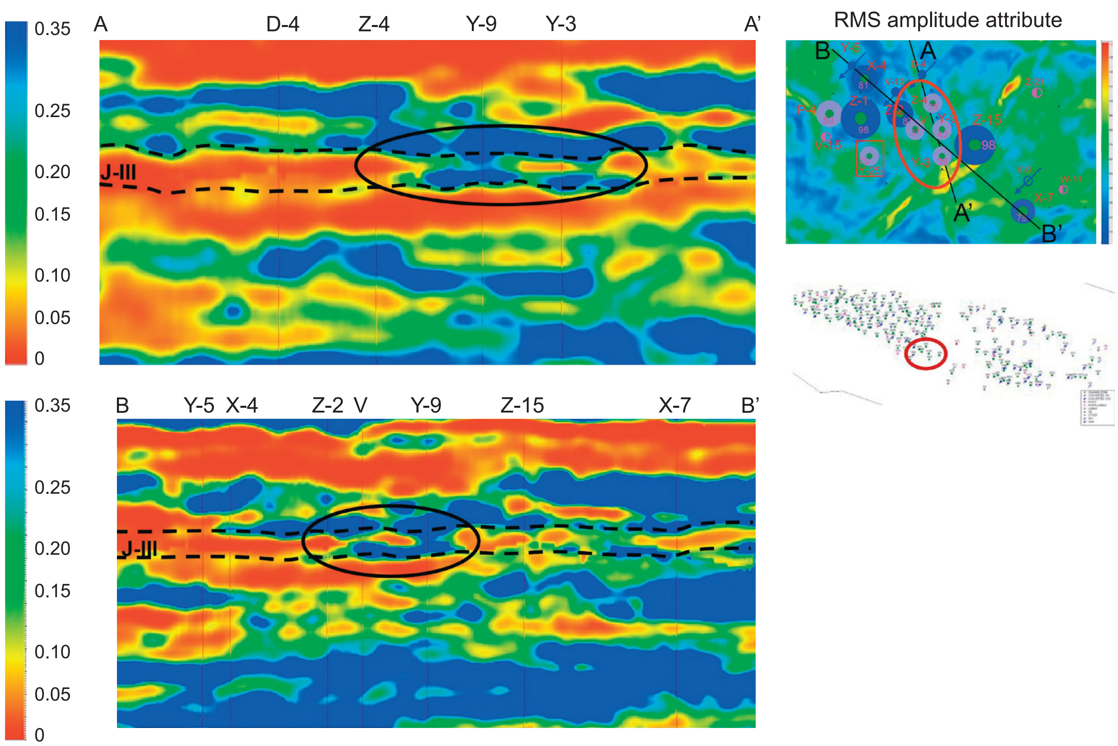

Fig. 7. Cross-sectional seismic inversion of sandy clay rocks.

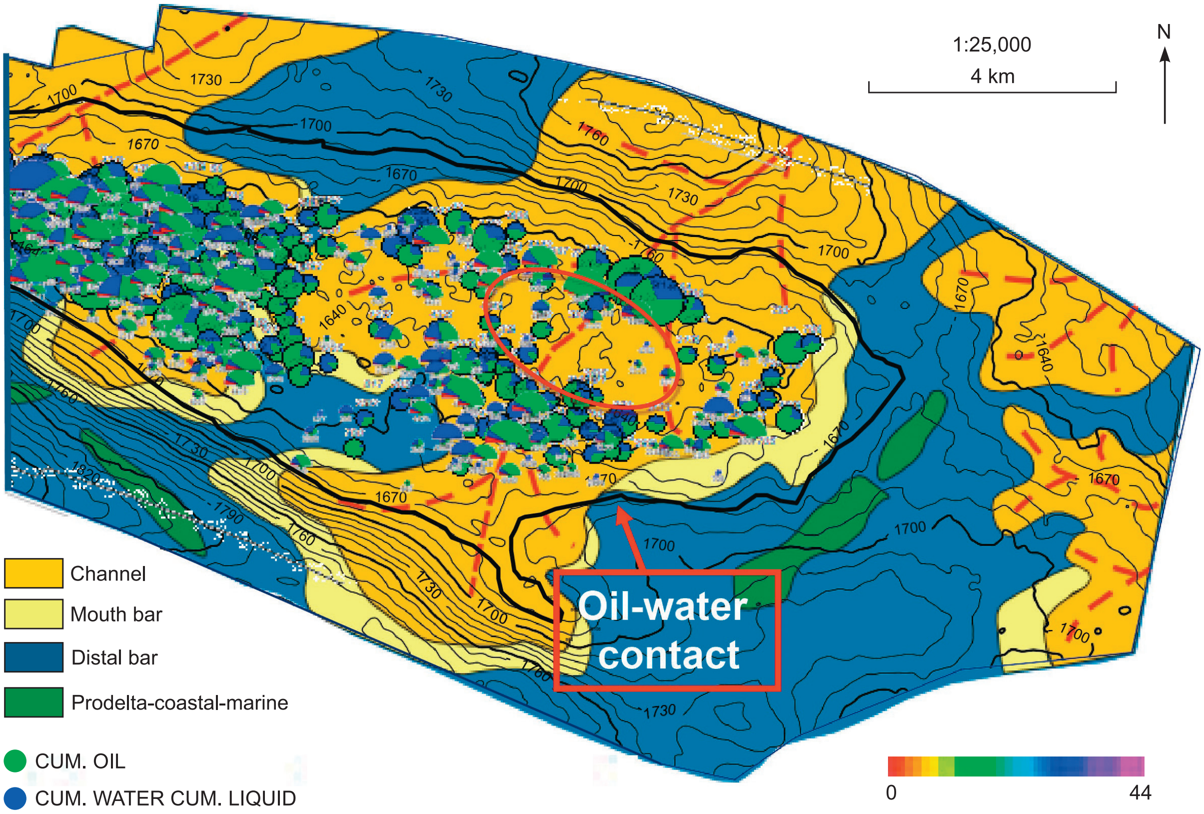

Fig. 8. Overlay map of the accumulated production, sedimentary microfacies, and structure of horizon J-III.

Selection of potential sites

Based on previous studies, a geological model (Ibragimov et al., 2019) was constructed to estimate the volumes and distributions of remaining oil per reservoir interval (Fig. 9). The distributions of initial oil shown in the maps suggest that the main production potential of horizon J-III is concentrated in the west and south, and this was confirmed by the cumulative well production (Fig. 10). The area of poor deposit development, concentrated in the east, is the future target area for recompleting deeper wells and drilling new wells.

A map of the locations and superpositions of favourable zones, with the distributions of drilled wells over the study area, was constructed according to the superposition of all of the identified potential sections in the reservoirs. Potential sections of high interest were divided into two major regions – the areas of the recompleted wells and of the new wells. Currently, there is a large proportion of idle and shut-in deeper wells, but their potentials for recompletion are mainly concentrated in the central part of the oil reservoir. The area of new wells is therefore primarily located along the edges of the oil reservoir, where there is interpreted to be a high remaining oil potential. The potential redevelopment area was calculated to be 17.69 km^2 for all layers and the proven undeveloped reserves for the J-III horizon were calculated to be 29.5 MMbbl.

RESULTS AND NEW WELL DEVELOPMENT SCENARIO

The first step that we recommend for recovering the remaining oil in the South Mangyshlak subbasin is to fully use the old well stock to recomplete wells for production from overlying horizons, which will provide quick and cost-effective potential sites. Our analysis of all shut-in and idle wells led to the selection of many wells suitable for recompletion from overlying horizons. As a result of analysing well dynamics, and in combination with potential sections, wells on horizon J-III were selected to recomplete from overlying horizons. According to the final proposal for horizon J-III, three wells are suitable for recompletion from overlying horizons and eight new wells are suitable for drilling in the southern part of the sub-basin (Fig. 11).

Using the map of the distribution of the proven undeveloped reserves (Fig. 12), new wells were proposed for each reservoir interval. Then, shut-in deeper wells were recommended for secondary utilisation to produce from the overlying horizons. This approach of generating a development plan is iterative and was based on the

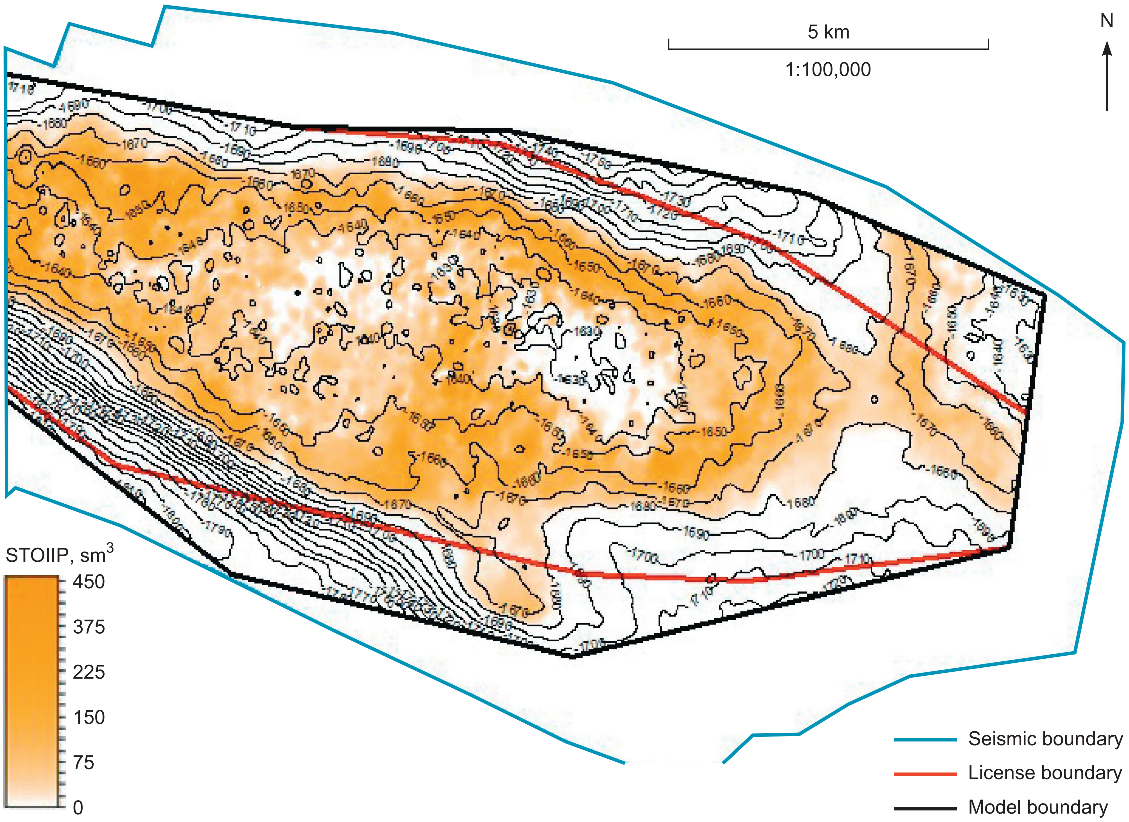

Fig. 9. Distribution of oil resources in horizon J-III.

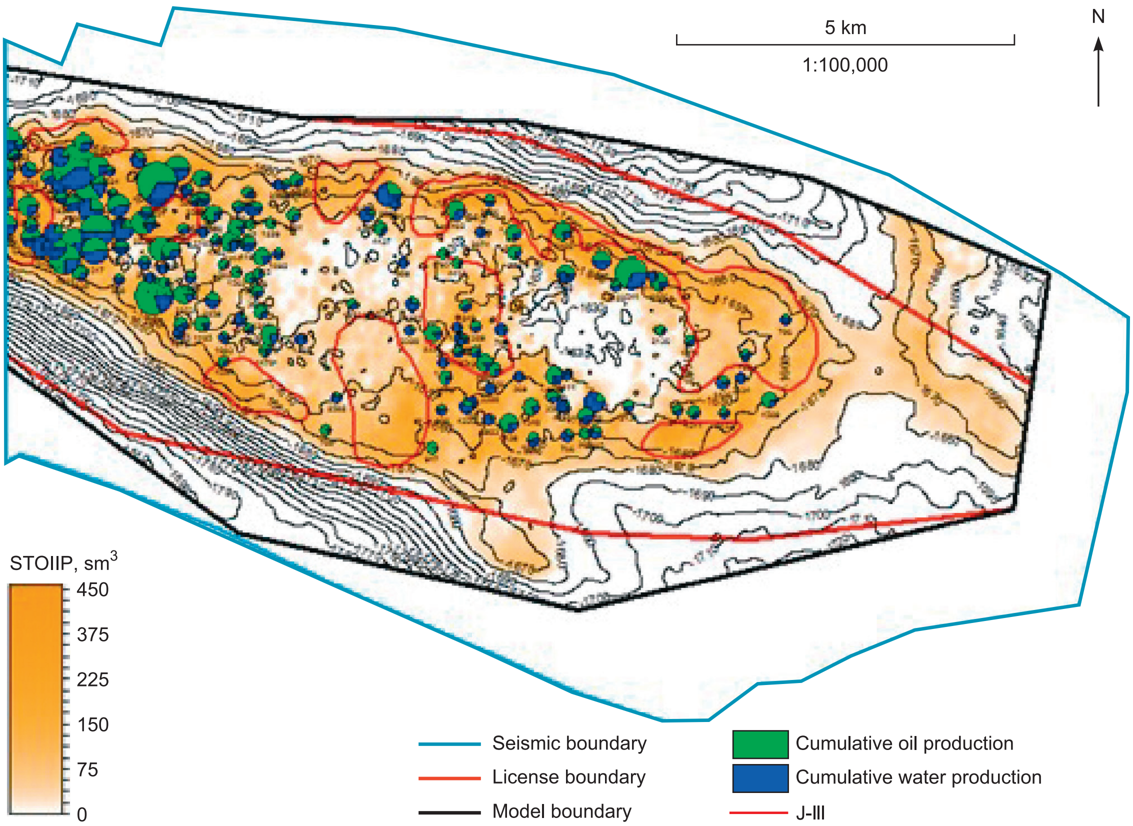

Fig. 10. Overlay map of cumulative production, structure, and oil resources in horizon J-III.

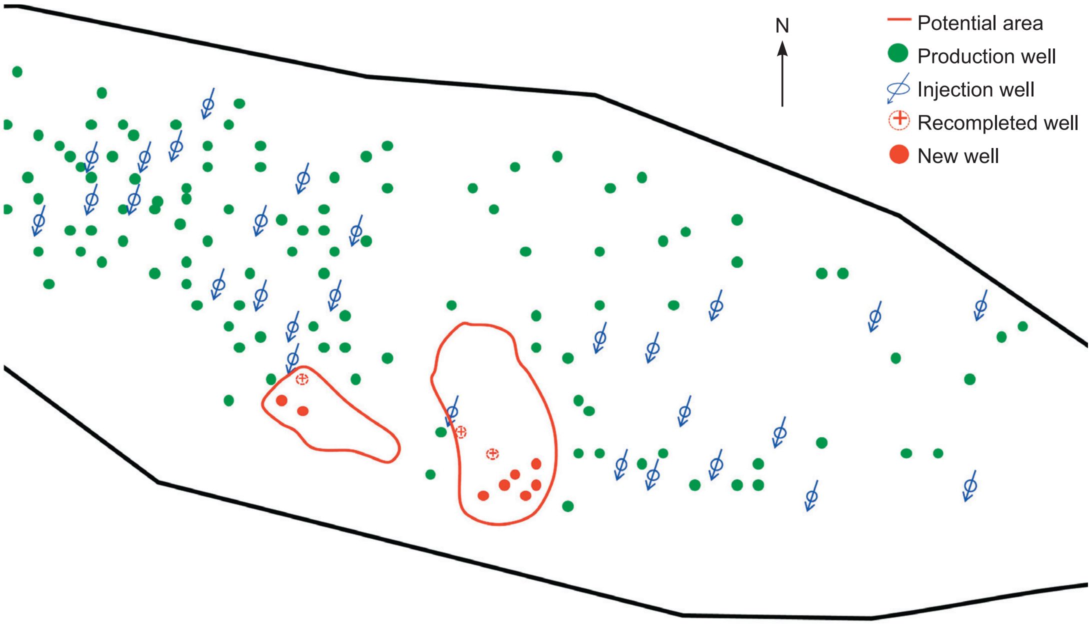

Fig. 11. Map of the distribution of potential areas and proposed new well locations.

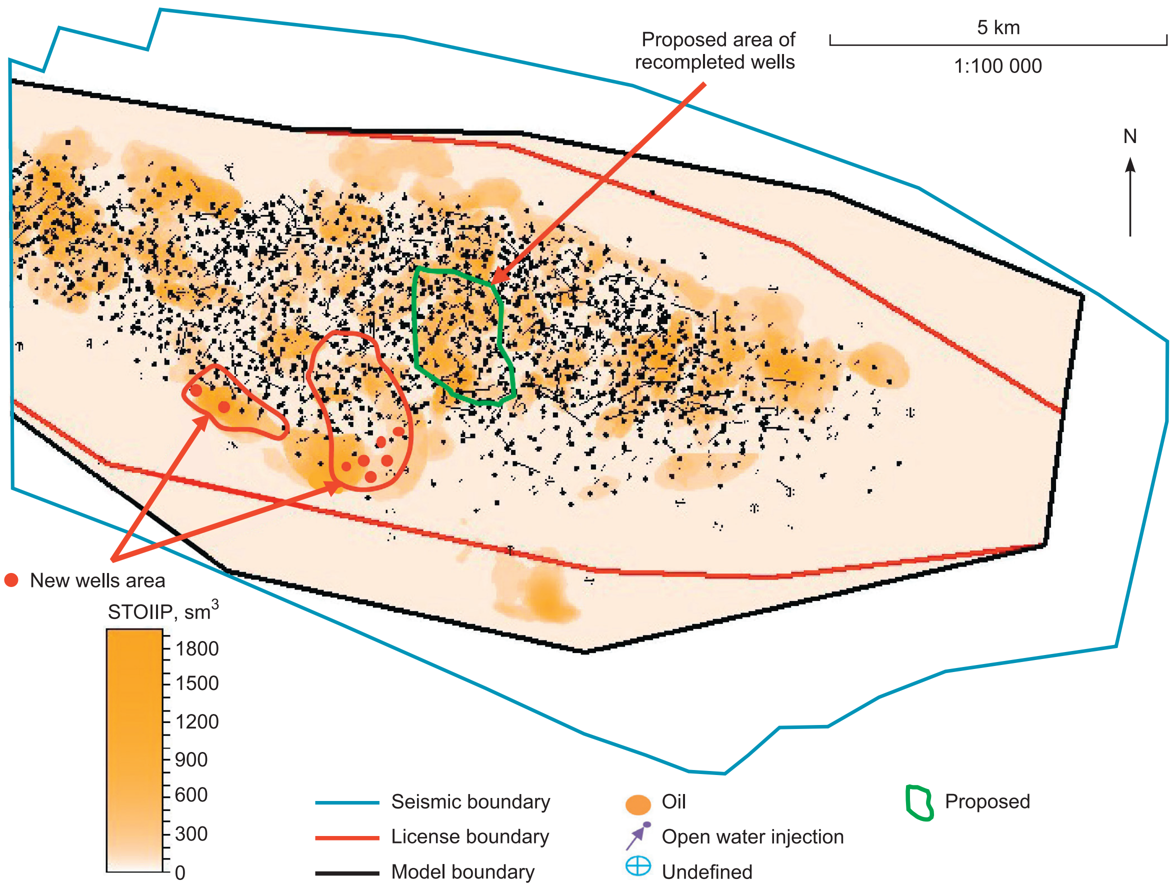

Fig. 12. Map of the locations of new wells superimposed by the new undeveloped resources in horizon J-III.

map of undeveloped reserves. To increase the chance for the future redevelopment of closely spaced wells, we recommend drilling as many horizons as possible during the development of new wells.

CONCLUSIONS

Seismic data were used to constrain a structural and geological model of the study area, which provided the basis for adjusting the developmental approach of the oil reservoir and for assessing the exploration potential of the area. A comprehensive study using seismic inversion attributes and sedimentary (micro) facies revealed that reservoirs in the South Mangyshlak subbasin are mainly composed of deltaic deposits. Deposition in the reservoir included deltaic and branched channel sand bodies; the thickness of the sandstones varies markedly in the study area, and the lateral connectivity of the reservoir is complex. The main target horizon, J-III, contains four 4-branched deltas and channel sand bodies that are spread in a wide, perpendicular strip, with the distribution and productivity of hydrocarbons being determined by the facies characteristics. There is potential for redevelopment of the field; specifically, the low-seismic-amplitude traps at the edges of the study area appear to have potential. Resources in the southern and central part of the area amount to 29.5 MMbbl. Therefore, it is necessary to drill new wells to rapidly develop these field reserves.

The new, integrated workflow proposed here should enable the operating company to efficiently review production enhancement opportunities within the bypassed zones of reservoir layers, whether targeting structural or stratigraphic oil zones. Moreover, new drilling and workover opportunities to access remaining oil along the edges of the main sand bodies and in discontinuous areas have been identified from their seismic attributes. We ranked these targets based on their expected flow rates, ultimate recoveries, and associated reservoir and operational risks. This approach also provides a means of developing an in-depth understanding and for conducting a detailed exploration of the known best-producing areas that have historically been successfully drilled within the field.

We thank BGP Inc., China National Petroleum Corporation for their data support and assistance during the project. We would also like to thank the geophysical adviser and editor-in-chief at First Break EAGE, European Association of Geoscientists and Engineers, Peter Rowbotham, for additional scientific review and language assistance.

REFERENCES

Aliyeva, E.H., 2009. Middle Caspian Mesozoic petroleum system – terrigenous source-rocks and carbonate reservoirs, in: Conf. Proc. 71st EAGE Conference and Exhibition incorporating SPE EUROPEC, doi: 10.3997/2214-4609.201400120.

Arslan, I., Rajabi, F., Ibrahima, F., 2019. Practical automated detection of remaining oil in mature fields using production and geology data, in: Proc. SPE Western Regional Meeting, San Jose, California (April 23–26, 2019), SPE-195321-MS, doi: 10.2118/195321-MS.

Avseth, P., Mukerji, T., Mavko, G., 2010. Quantitative Seismic Interpretation. Cambridge University Press, Cambridge, doi: 10.1017/CBO9780511600074.

Berkhout, A.J., 1993. Seismic reservoir characterization. Conf. Proc. 3rd Int. Congr. Brazilian Geophys. Soc., doi: 10.3997/2214-4609-pdb.324.1522

Brown, A.R., 1996. Seismic attributes and their classification. The Leading Edge15 (10), 1090, doi: 10.1190/1.1437208.

Cao, L., Xu, Y., Yu, J., 2005. Facies analysis with merged 3D seismic data, in: SEG Technical Program Expanded Abstract. SEG, Houston, pp. 739–742, doi: 10.1190/1.2144432.

Carter, D.C., 2003. 3-D seismic geomorphology: Insights into fluvial reservoir deposition and performance, Widuri field, Java Sea. AAPG Bull. 87, 909–934, doi: 10.1306/01300300183.

Chopra, S., Marfurt, K.J., 2005. Seismic attributes – a historical perspective. Geophysics 70 (5), 3–28, doi: 10.1190/1.2098670.

Chopra, S., Marfurt K.J., 2014. Churning seismic attributes with principal component, in: SEG Technical Program Expanded Abstract. SEG, Denver, pp. 2672–2676, doi: 10.1190/segam2014-0235.1.

Effimov, I., Downey, M.W., Threet, J.C., Morgans, W.A., 2001. Future hydrocarbon potential of Kazakhstan, Petroleum Provinces of the 21st Century. AAPG Mem. 74, 243–258.

El-Mowafy, H.Z., Marfurt, K.J., 2016. Quantitative seismic geomorphology of the middle Frio fluvial systems, south Texas, United States. AAPG Bull. 100 (4), 537–564, doi: 10.1306/02011615136.

Gunter, G.W., Finneran, J.M., Hartmann, D.J., Miller, J.D., 1997. Early determination of reservoir flow units using an integrated petrophysical method, in: Proc. SPE Annual Technical Conference and Exhibition. San Antonio, Texas, SPE-38679-MS, doi: 10.2118/38679-MS.

Harilal, Biswal, S.K., Sood, A., Rangachari V., 2008. Identification of reservoir facies within a carbonate and mixed carbonate-siliciclastic sequence: Application of seismic stratigraphy, seismic attributes, and 3D visualization. The Leading Edge 27 (1), 18–29, doi: 10.1190/1.2831675.

Ibragimov, R., Ovchinnikov, A., Burdakov, D., Romantsov, A., Sterlyagova, S., Darmaev, B., Zimin, S., 2019. Geology driven history match of Eastern Siberian halite cemented fluvial reservoir, in: Proc. SPE Abu Dhabi International Petroleum Exhibition and Conference, Abu Dhabi, UAE, SPE-197438-MS, doi: 10.2118/197438-MS.

Kazhegeldin, A.M., 1997. Oil and Gas Fields of Kazakhstan. Ministry of Ecology and Natural Resources, Almaty.

Kiritchkova, A.I., Timoshina, N.A., Menshikova, N.Y., 1983. Stratigraphy of the Jurassic deposits of Mangyshlak. Soviet Geology 11, 73–82.

Lechner, M., Iltukov, R., Mukushev, M.A., 2016. Multidisciplinary approach to improve reservoir management of a tidal-fluvial channel reservoir in Tasbulat Field, Kazakhstan, in: Conf. Proc. SPE Europec featured at 78th EAGE Conference and Exhibition, doi: 10.2118/180192-MS.

Muruthy, S.P., Ghosh, D.P., 2018. Integration of seismic attributes, petrophysics, and rock physics for depositional environment and facies characterization. Conf. Proc. EAGE-HAGI 1st Asia Pacific Meeting on Near Surface Geoscience and Engineering, doi: 10.3997/2214-4609.201800444.

Pennington, W.D., 1997. Seismic petrophysics: an applied science for reservoir geophysics. The Leading Earge 16 (3), 241–244, doi: 10.1190/1.1437608.

Posamentier, H.W., 2000. Seismic stratigraphy into the next millennium: a focus on 3D seismic data. AAPG Annual Convention Program, A118.

Smale, J.L., Dropkin, M., Bhattacharyya, D., Korsotyshevsky, M., Pronin, A., Gaisina, S., 1997. Middle to Upper Jurassic clastic reservoirs in the Petroleum Basins of Western Kazakhstan: parasequence architecture controls on hydrocarbon production. AAPG Int. Conf. Exhib. 81, 1412–1413.

Soloviev, V., Gelman, V., Paduchih, V., Cherenov, V., Solntsev, B., 2017. Geological structure and oil and gas potential of the platform part of the Caspian Sea. Neftegaz.ru, https://neftegaz.ru/science/development/331536-geologicheskoe-stroenie-i-neftegazonosnost-platformennoy-chasti-kaspiyskogo-morya/.

Tang, M., Zhang, K., Huang, J., Lu, S., 2019. Facies and the architecture of estuarine tidal bar in the Lower Cretaceous McMurray Formation, Central Athabasca Oil Sands, Alberta, Canada. Energies 12 (9), 1769, doi: 10.3390/en12091769.

Ulmishek, G.F., 1990. Uzen field – U.S.S.R., Middle Caspian Basin, South Mangyshlak region. Structural Traps IV: Tectonic and Nontectonic Fold Traps. AAPG Spec. Vol., 281–297.

Ulmishek, G.F., 2001. Petroleum geology and resources of the Middle Caspian Basin, Former Soviet Union. U.S. Geol. Surv. Bull. 2201-a.

Walls, J., Dvorkin, J., Carr, M., 2004. Well logs and rock physics in seismic reservoir characterization, in: Proc. SPE Offshore Technology Conference. Houston, Texas, OTC-16921-MS, doi: 10.4043/16921-MS.

Wu, J., Zhou, D., Lv, D., Niu, C., He, D., Li, G., L., Wang, X., 2014. Structural interpretation of inner buried hill under restricted data availability – A case study in KL-X Area, Bohai Bay Basin in: SEG Technical Program Expanded Abstract. SEG, Denver, pp. 1689–1693, doi: 10.1190/segam2014-1096.1.

Zabihi Naeini, E., Exley, R., 2016. Quantitative interpretation using facies based seismic inversion, in: SEG Technical Program Expanded Abstracts, 2906–2910, doi: 10.1190/segam2016-13709660.1.

Zhang, Y., Wang, H., Hu, X., Zhang, X., Pu, F., Gao, Y., Fan, E., 2016. Reservoir modelling of complex lithologies with sparse wells: a case from a oilfield in Shijiutuo uplift, Bohai Bay Basin. Oil Gas Geol. 7 (3), 450–456.

Zudakina Y.A., Yefremova L.N., Vorontsova G.I., Rmyantsev A.A., 1981. Effect of conditions of sedimentation and of post-sedimentary alterations on reservoir properties of polymict sandstones of the Uzen Field. Petrol. Geol. 17 (7), 286–290.

Поступила в редакцию 12 февраля 2021 г.,
принята в печать 6 октября 2021 г.